

Residual Stress Analysis of Friction Stir Processed AA6061

M. Iordachescu¹, J. Ruiz Hervías¹, D. Iordachescu², E. Scutelnicu³, J. A. Porro²

¹ Ciencia de Materiales Dep., ETSI Caminos, Canales y Puertos, Universidad Politécnica de Madrid, C/ Profesor Aranguren s/n, 28040 Madrid, Spain

² Centro Láser-UPM Universidad Politécnica de Madrid, Ctra.de Valencia, km. 7,3; Campus Sur U.P.M. (Edificio "La Arboleda"), 28031 Madrid, Spain

³ Robotics and Welding Dep., "Dunarea de Jos" University of Galati, 47 Domneasca St., 800008, Galati, Romania

E-mail: miordachescu@mater.upm.es

Abstract

Currently, after appropriate heat treatments, the 6xxx aluminium alloys are used in a variety of applications including aircraft fuselage skins and automobile body panels and bumpers, instead of more expensive 2xxx or 7xxx alloys. The paper presents the results of the residual stress analysis in case of Friction Stir Processing - FSP of AA6061-T4 plates, 10 mm thickness, demonstrating the process ability to locally modify the base metal properties. The residual stresses, DRX depicted, are correlated with the microstructure and hardness results.

Introduction

Nowadays, AA6061-T4 is one of the primary choices for light plane skin, which needs moderately high yield strength and hardness to minimize ground damage from stones, debris, mechanics' tools, and general handling [1]. New techniques as solid-state Friction Stir Welding – FSW are currently used for obtaining AA6061-T4 qualitative joints. Although the welding may produce high tensile stresses (up to the yield stress) balanced by lower compressive residual stresses elsewhere in the component, FSW results in a much lower distortion and residual stresses owing to the low heat input characteristic of the process [2], [3].

Recently, a derivative from FSW, the so called Friction Stir Processing – FSP was proved as being useful for inducing directed, localized, and controlled materials properties in any arbitrary location of components [4]. The microstructure of the processed layer is complex and highly dependent on the position within the processed zone. This is due to the large local variations in the plastic flow, and to the thermal history resulted from the material interaction with the processing tool.

To friction process a location within a plate, a specially designed cylindrical tool (Figure 1) is rotated and plunged into the selected area. The tool has a small diameter threaded

pin concentric with a larger diameter shoulder. When the rotating pin contacts the surface, its friction rapidly heats and softens a small column of metal. The tool shoulder and the length of the entry probe control the penetration depth. When the shoulder contacts the metal surface, its rotation creates additional frictional heat and plasticizes a larger cylindrical metal column around the inserted pin. The shoulder provides a forging force that contains the upward metal flow caused by the tool pin. During FSP, the processed area and the tool are moved relative to each other such that the tool traverses, with overlapping passes, until the entire selected area is processed. The rotating tool provides a continuing hot working action, plasticizing the metal within a narrow zone, whilst transporting material from the leading face of the pin to its trailing edge.

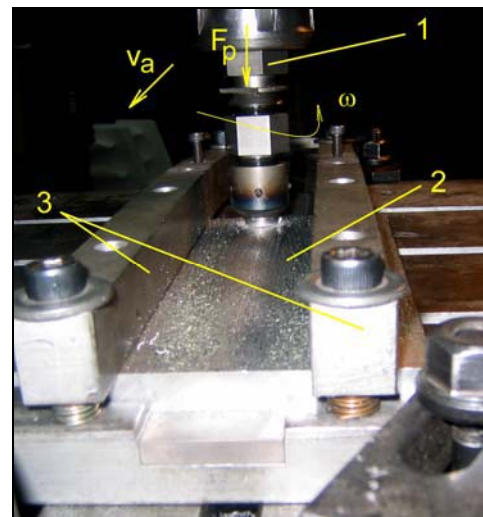


Figure 1: FSP of AA6061-T4 alloy: 1) processing tool; 2) AA6061-T4 probe-plate; 3) clamping device; F_p – pressing force; v_a – travel speed; ω - rotation speed.

The process is carried out in solid state at low temperature, typically below 0.3 of the aluminium alloys fusion temperature (T_f) [2], [5]. The processed zone is deformed and under the thermal effect recovers or recrystallizes, forming a defect-free recrystallized fine grain microstructure [2].

The thickness of the modified layer is directly related to the friction pressure, whereas it is inversely affected by the rotation speed of friction tool and the traverse speed. The microstructure and properties of the modified layer depend on the amount of frictional heat generated by processing [2], [6].

The peculiar behaviour of cold rolled AA6061-T4 alloy after FSP was investigated through microstructural analysis, and HV microhardness tests, respectively. The correlation between the features of the residual stresses field and the material flow in the processed zone was of interest, as too.

Experimental Procedure

The research was conducted on cold rolled AA6061-T4 plates, of 10 mm thickness, and the chemical composition is presented in Table 1. Samples of 200x300 mm were longitudinally friction stir processed using the “cold working” conditions ($\omega/v_a = 3.5$, where ω is the rotation speed, [rpm] and v_a - travel speed, [mm/min] [6]).

Table 1: AA6061 - Chemical composition

AA6061 - Chemical composition (wt %)								
Si	Fe	Cu	Mn	Mg	Cr	Zn	Ti	Al
0.66	0.25	0.31	0.08	0.99	0.16	0.01	0.02	bal

FSP tool characteristics and the process main operating parameters as friction pressure (tool up-setting force), tool rotation and travel speed are presented in Table 2.

Table 2: FSP tool characteristics and process parameters

Shoulder diameter [mm]	15
Pin diameter [mm]	5
Pin length [mm]	4
Rotation speed ω , [rpm]	1120
Travel speed v_a , [mm/min]	320
Friction pressure (up-setting force), [kN]	25
Pin angle, [$^\circ$]	2.5

Standard metallographic procedures were followed for the macro and microstructural analysis. A modified Keller's reagent was used for etching. Observations of plastic deformation, material flow and microstructure were performed by using optical microscopy.

Vickers microhardness measurements were performed on processed layers cross-sections by using a microhardness tester at 100 g load and 15 s dwell time. The X-ray, peak shift $\sin 2\psi$, technique with $\text{CrK}\alpha$ radiation was used to determine the residual stresses by measuring the surface strains.

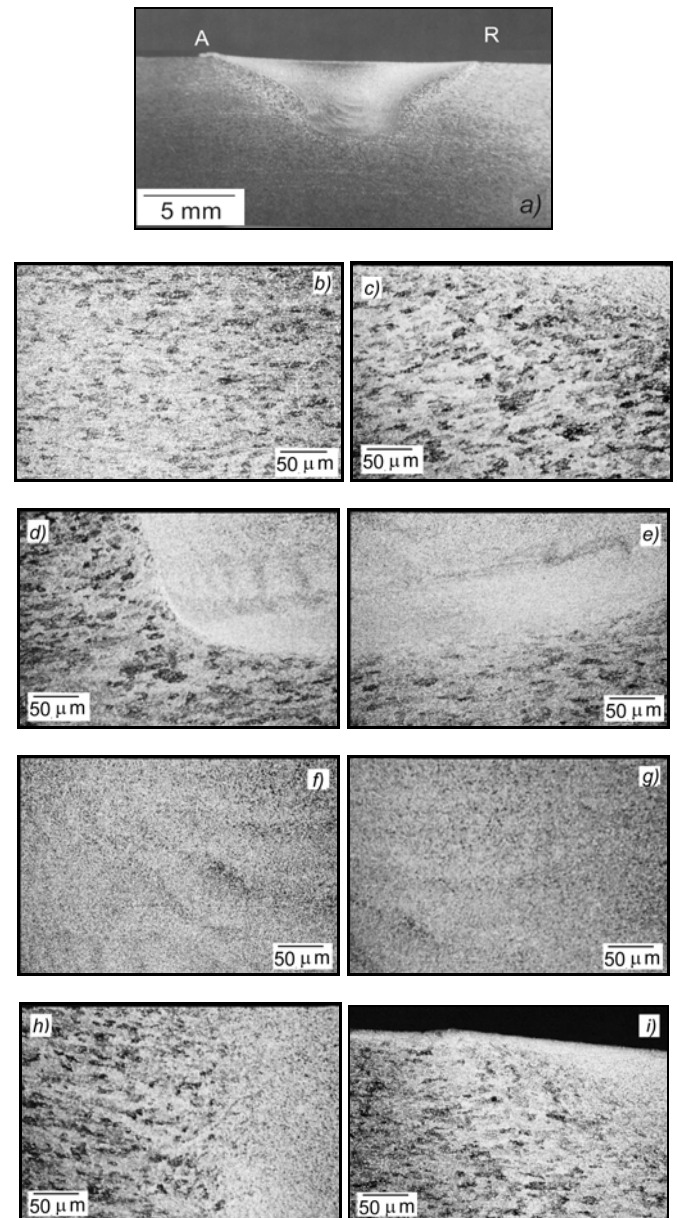


Figure 2: Typical features of all different zones in a friction stir processed single layer cross-section of AA6061-T4:

a) processed layer macrostructure; b) base metal (BM) optical microstructure; c) optical microstructure of HAZ; d) optical microstructure of HAZ and TMAZ in the advancing side of the processing tool; e) optical microstructure of the bottom part of the processed zone, TMAZ and HAZ respectively; f) optical microstructure of the SZ in the advancing side of the tool; g) optical microstructure of the SZ corresponding to the processed layer nugget; h) optical microstructure of HAZ and TMAZ in the upper part of the processing tool; i) optical microstructure of HAZ and TMAZ close to the surface of the processed layer.

Results and Discussion

Material Flow and Microstructure

The base metal (BM), Figure 2, b and stirred zone (SZ) microstructure of AA 6061-T4, consist of Al solid solution dendrites along with coarse silicon and intermetallic phases. Grain size varies from the top to the bottom as well as from the advancing to the retreating side. The differences in grain size likely are associated with differences in both peak temperature and time of application of temperature.

In Figure 2c-i, both the Thermo-Mechanically Affected Zone (TMAZ), (which includes the nugget and plastically deformed grains), and the Heat Affected Zone (HAZ), respectively, are presented. In FSW/FSP, the processing technique called “cold working” does not generate the melting of the nugget. Due to these “cold working” conditions used for processing the aluminium alloy, the concentric rings of the nugget are not clearly distinguishable on the macrostructure presented in Figure 2a. Moreover, the nugget appendage does not occur. The analyzed case corresponds to a processed layer which has a “basin shape” form.

Figures 2b-i show the typical features of different microstructural zones located in a single processed layer cross-section of AA 6061-T4. The micrographs show that the microstructure of the processed layer is complex and highly dependent on the position within the processed zone. This result arises because of the large local variations in the plastic flow and from the thermal history resulted from the material interaction with the tool.

The microstructure in SZ is characterized by refined grains in a discrete series of bands and some precipitate mainly distributed at the grain boundaries. The nugget zone grains suggest effective strains together with a microstructural evolution that occurs by a combination of hot working and a dynamic recovery or recrystallization. The temperature reached in the nugget zone is known as being situated in the range of 450°C for the 6061-Al alloy [2], [5]. Distinct precipitates and coarsened grains are observed in HAZ regions, where the grains are severely coarsened by FSP (Figures 2c,d,e,h,i).

The characteristic annular-banded structure is observed to be asymmetric and more obvious on the advancing side (A) of processed zone as shown in Figures 2a,d,f. A severe deformation occurred along the top surface of the processed layer where the shoulder of the tool is in contact with the material (Figure 2i). The flow lines from Figures 2d,f seem to represent plastic deformation increments that develop as the rotating tool moves through the processing line.

It is well known that the material is transported from A to the retreating side (R), the results matches the Colligan’s reports [5], which showed that due to the threaded pin tool, the material from the upper part of the processed zone is pressed down (Figure 2h), whereas the material from the lower part of the processed zone is moved toward the top surface (Figure 2d). The plasticized material may travel many cycles around the tool before being redeposited.

Hardness Distribution in the Processed Material

Figure 3 shows the typical microhardness distribution of the single layer processed cross-section of AA6061-T4 alloy.

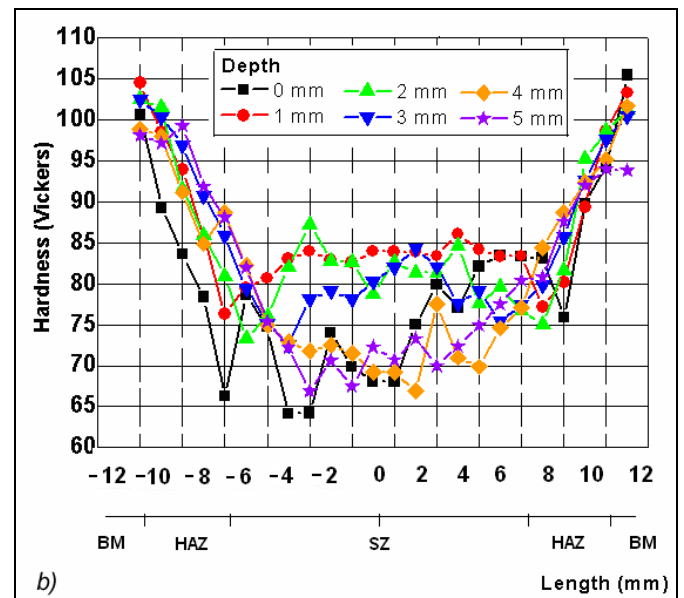


Figure 3: HV test of the FSP cross-section layer in case of AA6061-T4: a) macrostructure with microhardness imprints; b) microhardness profile.

The microhardness of the SZ is considerably lower than that of the parent metal (which is situated in a range of 95-105 HV, according to Figure 3), varying from the top to the bottom of the processed layer.

Generally, the hardness depends on the precipitate distribution rather than grain size. It is likely that low hardness in the SZ can be attributed to dissolution of the precipitate during FSP. The width of this soft zone depends on peak temperature and thermal cycle duration. Moreover, the retention of the processed region at a certain temperature

for prolonged period results in considerable softening. This is due to the temperature range going by about 450°C within the SZ of AA 6XXX aluminium alloys [2], [7]-[8]. In case of AA 6061 aluminium alloy, this temperature is sufficient to dissolve all precipitates; when the processing ends, the cooling rate is sufficiently rapid to retain alloying elements in saturated solid solution.

An abrupt change in hardness between parent metal and HAZ is evident at a distance of ± 7 mm from the friction stir processed layer centre. Moreover, the resulted wide region of HAZ (Figure 3a) is due to the high thermal conductivity of the base metal. At a distance of about ± 7 mm from the centre of the processed layer, the hardness dips to a value of about 65 HV, and 70 HV for advancing and retreating side, respectively (Figure 3b). This indicates that the naturally age hardened parent metal has been overaged as a result of the processing induced frictional heat. HAZ softening is explained by the coarsening of the metastable phases due to temperature rise during processing as a result of frictional heat (Figure 2c,d). The HAZ loss of hardness can be due to the dissolution or coarsening of Mg_2Si phase, the main strengthening phase in Al-Mg-Si alloys.

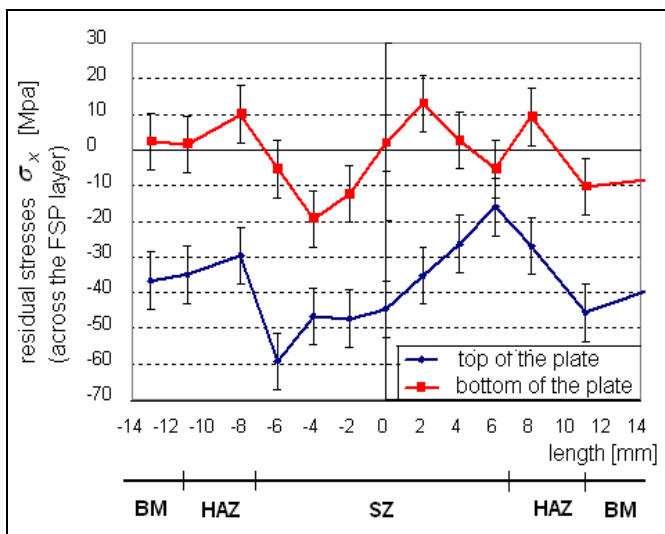


Figure 4: Residual stresses profile across a FSP layer in case of AA6061-T4.

Residual stress distribution

Conventional X-rays have a penetration depth of several μm up to some $10\mu m$ in case of aluminium. Thus, using conventional X-rays, the residual stresses at the front and the bottom side of the friction stir processed layer can be determined. The resolution in the in-plane direction was approximately 2 mm. The measurements were performed on a Ψ – diffractometer using the $\sin^2\psi$ –method.

The results of the residual stress analyses reveal that the residual stress distribution is inhomogeneous in the

transverse direction of the processed layer as well as across the thickness of it.

In transverse direction of the processed layer, in all specimen examined, “M” like stress distribution resulted on the plate top surface.

On the FSP top surface, only compressive residual stresses were found. The maximum values of these are located at the HAZ-SZ interface (Figure 4). The residual stresses in other zones are smaller than these maximum values, and the parent material adjacent to the HAZ, as well as the processed layer contain small values of compressive residual stresses. With the depth increase, the “M” like stress distribution is still found at the bottom part of the processed plate, but the residual stresses values are close to those corresponding to the initial stress state of the sheet material (Figure 4), and are both tensile and compressive.

The influence of FSP tool and process parameters, corresponding to “cold working” conditions on the residual stress distribution is explained by the increased distance between the tensile stress peaks. The magnitude of the tensile residual stresses reached in the HAZ is caused by the process heat input; the resulted wide HAZ and the lower material cooling rate produced the relatively low magnitude of the compressive residual stresses in the processed zone. The compressive stresses can be beneficial for reducing the crack propagation speed.

Conclusions

Several conclusions can be underlined about FSP of AA6061-T4:

- ✓ The process makes an effective surface modification.
- ✓ The material plastic deformation, flow and mechanical mixing exhibit distinctly asymmetric characteristics at advancing, and retreating side zones.
- ✓ The hardness loss by friction stir processing of AA6061-T4 alloy depends on the process parameters, tool rotating and advancing speed; the width of this soft zone depends on peak temperature and thermal cycle duration. The material softening is due to dissolution or coarsening of Mg_2Si phase precipitate during FSP.
- ✓ The resulted wide heat affected zone and the lower material cooling rate produced the relatively low magnitude of compressive residual stresses in the processed zone. The compressive stresses can be beneficial for reducing the crack propagation speed.

- ✓ The process addresses the industry as surface repairing technique in case of different types of flaws.

References

- [1] L. P Troeger, and E. A. Starke, *Microstructural and Mechanical Characterization of a Superplastic 6xxx Aluminium Alloy*, Materials Science and Engineering, A277, 102-113, 2000.
- [2] R. S. Mishra, and Z. Y. Ma, *Friction stir welding and processing*, Materials Science and Engineering R 50 (2005) 1–78, Elsevier, 2005.
- [3] W. M. Thomas, et. al., *Friction Stir Butt Welding*, International patent Application PCT/GB92/02203, GB Patent Application 9125978.8, US Patent 5.460.317, 6 December 1991.
- [4] M. Iordachescu, D. Iordachescu, E. Scutelnicu, P. Vilaca, J. L. Ocana, *Aluminium friction stir processing – roughness vs. macro/microscopically results*, Welding in the World, Vol. 51, Sp. Iss., 441-448, 2007.
- [5] K. Colligan, *Material Flow behaviour during Friction Stir Welding of Aluminium*, Welding Journal, 75(7), 229s-237s, 1999.
- [6] P. Vilaça, J. P. Santos, A. Góis, and L. Quintino, *Joining Aluminium Alloys Dissimilar in Thickness by Friction Stir Welding and Fusion Processes*, Welding in the World, Vol. 49, No. 3/4, 56-62, 2005.
- [7] P. Staron, M. Kocak, S. Williams, and A. Wescott, *Residual stress in friction stir-welded Al sheets*, Physica B 350, e491–e493, Elsevier, 2004.
- [8] C. Dalle Donne, E. Lima, J. Wegener, A. Pyzalla, and T. Buslaps, *Investigations on Residual Stresses in Friction Stir Welds*, 3rd International Symposium on Friction Stir Welding, Kobe, Japan, TWI (UK), CD-ROM, 27 - 28 September 2001.